Photoemission study of the electronic structure of $CrCl_3$ and $RuCl_3$ compounds

I. Pollini
Dipartimento di Fisica dell'Università di Milano, Via Celoria 16, 20133 Milano, Italy
(Received 15 November 1993; revised manuscript received 17 February 1994)

X-ray and ultraviolet photoelectron spectra of the valence band and core levels of $CrCl_3$ and α-$RuCl_3$ crystals have been performed in order to study their electronic structure. It is found that the $3d$ and $4d$ states of the transition metal and the $3p$ states of the chlorine contribute to the valence-band structure. The valence band consists of overlapping Cr $3d$ and Cl $3p$ states in $CrCl_3$, while a narrow Ru $4d$ band is separated by 2–2.5 eV from the top of the Cl $3p$ valence states in $RuCl_3$. Photoemission, photoconductivity, and optical spectra indicate that in $CrCl_3$ and $RuCl_3$ the energy gap involves d-d Coulomb and exchange interactions on the transition-metal atom. On this basis, the main $3d$- and $4d$-emission structures are assigned to unscreened $3d^2$ and $4d^4$ hole states within the framework of the Mott-Hubbard model.

I. INTRODUCTION

The electronic properties of transition-metal compounds (TMC's) have been the subject of many optical[1–4] and photoemission[5–10] studies for their fundamental importance. One of the most controversial topics has been the character of the valence and conduction electron states and the origin of band gaps in these materials. The attempt to treat the electrons in TMC's by the Bloch-Wilson band theory leads to partially filled bands, implying metallic conductivity for the compounds.[11,12] This is contrary to the experimental facts and has required some improvement of the theory. Self-consistent one-electron band-structure descriptions of their electronic properties break down because of strong electron correlations. As shown by Mott-Hubbard theory (MH),[13,14] a large d-d Coulomb correlation energy U (Coulomb repulsion energy between two electrons with opposite spin on the same site) introduces an energy gap in the d states, which explains, at least qualitatively, the insulating character of many TMC's. Another possibility is that there is a large gap in the d states due to electron correlation, but that the energy gap corresponds to charge-transfer transitions from the anion p-valence band to empty d states (p-d gap). This interpretation resulted from recent theoretical and experimental work largely based on NiO and Ni halides.[15,16] Recently, Zaanen, Sawatzky, and Allen (ZSA) presented a model for classifying TMC's in terms of U (Coulomb and exchange interaction), Δ (charge transfer energy), and W, the width of the anion valence band. In the simplest picture, if Δ is smaller than U, band-gap excitations consist of a transfer of electrons from the ligands to the cations, and the compound is in the charge transfer regime. On the other hand, if U smaller than Δ, band-gap excitations are intercationic $d \rightarrow d$ transitions, and the compound is in the MH regime. In real materials, the boundaries between the regions are smeared out due to cation-anion hybridization.[17]

The ZSA model predicts that the band gap (E_G) will be a d-d gap for Ti, V, and Cr oxides, and p-d gap for Cu and Ni halides.[18,19] There is, however, one difficulty: although the model is useful for predicting the systematics in band gaps of TMC's the experimental determination of the energy gap E_G is not easy. The optical spectra clearly show exciton peaks, but it is difficult to deduce from the spectra precise values of E_G for the charge transfer transitions (from ligand p band to cation d states) or, in general, to obtain from these methods precise information about the conductivity energy gap. As pointed out by Ronda, Arends, and Haas[3] the most reliable methods for determining E_G are the comparison of direct and inverse photoemission[18,20,21] or better, photoconductivity measurements, and even so, considerable discrepancy can be found between the calculated value of the energy gap E_G and the observed conductivity gap (see Table I of Ref. 3).

In this paper we report an XPS (x-ray photoelectron spectroscopy) study of the valence bands and core levels in $CrCl_3$ and $RuCl_3$ materials together with photoconductivity, optical, and ultraviolet photoemission spectra in order to study the nature of the energy gap in these materials.

XPS core-level spectra of $RuCl_3$ are also compared to new electron-loss spectroscopy results, where a plasmon structure is observed around 23 eV.

$CrCl_3$ has a hexagonal unit cell with $a = 5.952$ Å and $c = 17.47$ Å below 238 K.[22] The low-temperature structure of $CrCl_3$ has a rhombohedral unit cell with parameters $a = 5.942$ and 17.333 Å. The space group of $CrCl_3$ is C_{2h}^3 (monoclinic, four formula units per unit cell) above 240 K and C_{2i}^3 (rhombohedral, two formula units per unit cell) at lower temperature.[23]

The lattice consists of stacks of "sandwiches" formed by a hexagonal network of chromium ions between two layers of chlorine ions. The difference between the two structures results from the chlorine packing, which is fcc in the monoclinic and hcp in the rhombohedral form. The adjacent sandwiches are bonded by weak van der Waals interactions.

Ruthenium chloride is a layered compound of interesting fundamental properties and increasing importance in surface science and chemistry. Infrared and optical prop-

erties[24] together with transport experiments[25] had given some information about its fundamental electronic properties: it is a semiconductor with a energy gap of about 1 eV. The magnetic susceptibility shows that $RuCl_3$ is antiferromagnetic below $T_N = 13$ K.[26] As for the importance of $RuCl_3$ in material science studies, one only needs reminding of its catalytic properties[27] and its applications to photoelectrochemical devices,[28] where it is employed as an adsorbate on semiconductor surfaces. $RuCl_3$ is also used in the production of RuO_2 thin films which are used in electronic devices.[29]

Recent investigations by XPS have been carried out on samples of ruthenium chloride commercial powder.[30] α-$RuCl_3$ has the high-temperature crystal structure of $CrCl_3$ [C_{2h}^3, monoclinic, four formula units per unit cell above 240 K (Refs. 31 and 32)].

In $RuCl_3$ as in $CrCl_3$, the bonding is mainly ionic within the layers, while the stacking of adjacent layers is due to van der Waals forces. Inside the layers, the metal locations forms a hexagonal array and each Ru^{3+} site, with an electronic configuration $4d^5$, is octahedrally coordinated to its nearest-neighbor chloride ligands: the metal $4d$ states split into two subbands, the lower t_{2g} and the higher e_g.

The $4d$ transition-metal ions are more covalently bonded than in the $3d$ series and, roughly speaking, this means that the metal d electrons approach close to the ligand electrons and hence experience a stronger crystal field. For a $4d^5$ configuration the e_g levels are empty since up to six of the possible ten transition-metal d electrons can be accommodated in the lower t_{2g} levels; Hund's rule relaxes and the Ru^{3+} ion has a low spin ground state ($^2T_2$).

Generally the $3d$ transition-metal compounds are found to be high spin. Low-spin situations occur if the ligand field splittings are large or the charge transfer energy is small. This is different from the $4d$ transition-metal compounds where low-spin situations are much more common because of the more diffuse character of the $4d$ orbitals.

II. EXPERIMENT

The anhydrous form of $CrCl_3$ has been prepared by direct chlorination of the metal ion in a flow system at about 950 °C. At this high temperature the rather inert violet form of $CrCl_3$ is usually obtained. The crystals are pink-violet colored, lustrous, and very stable.

The anhydrous form of α-$RuCl_3$ has been prepared by direct chlorination of the metal ion in the presence of CO at about 750 °C. The purity of the starting materials (Ru metal powder and Cl_2 gas) was greater than 99.9%. The crystals (3×5 mm^2) are black, lustrous, and very stable with thicknesses between 5 and 50 μm. The state of crystallinity of $CrCl_3$ and $RuCl_3$ has been controlled by performing high-energy (220 keV) electron diffraction measurements by means of a electron microscope apparatus.[2] The incident beam is directed perpendicular to the surface of the crystals (thickness ~ 100 nm). The result of the Bragg diffraction pattern for $RuCl_3$ is presented in Fig. 1. The hexagonal symmetry of the electron diffraction pattern is observed with reflections $(h,k,0)$.

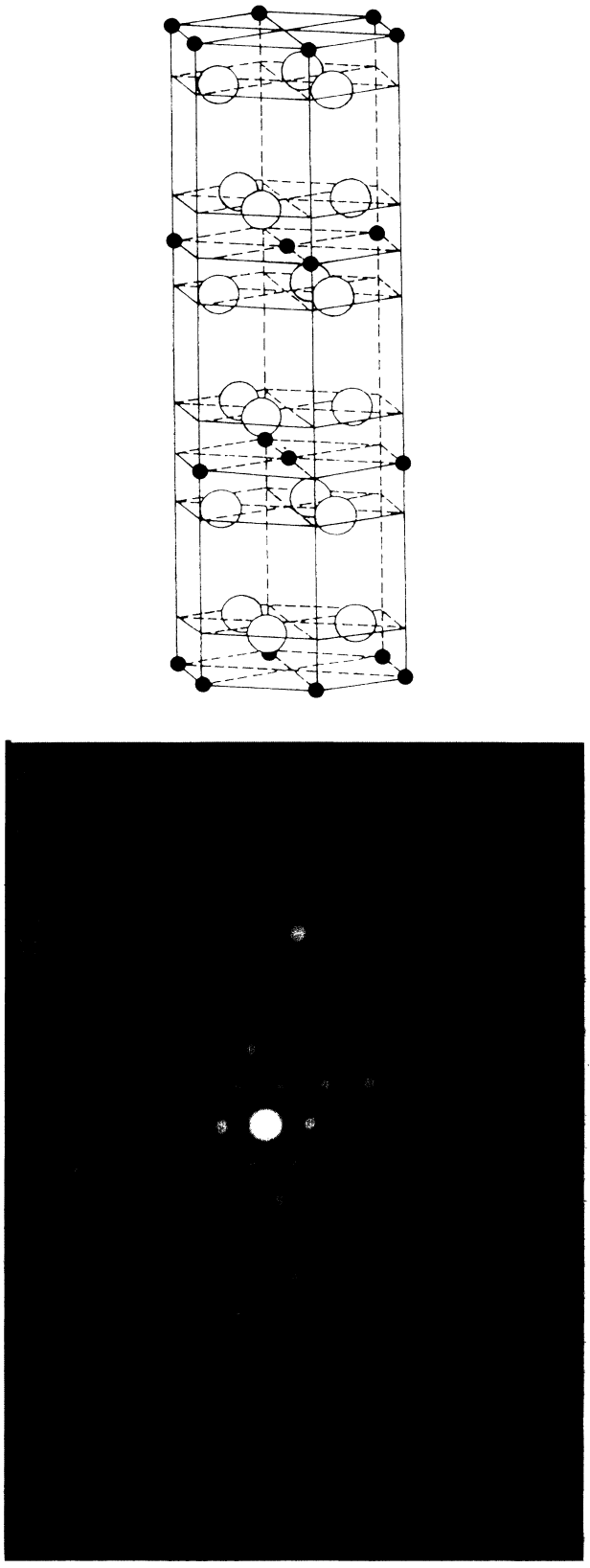

FIG. 1. High-energy (200 kV) electron Bragg diffraction patterns of crystals of α-$RuCl_3$. The monochromatic electron beam was incident on the crystal surface along the c axis. In the inset the structure of $CrCl_3$ and $RuCl_3$ crystals shows the octahedral environment of the metal (●, Cr, Ru; ○, Cl).

The XPS experiments were performed with a Vacuum Generators ESCALAB MKII system, equipped with a monochromatized Al $K\alpha$ x-ray source ($\hbar\omega = 1486.6$ eV); the total instrumental resolution was about 1 eV. The UPS (ultraviolet photoelectron spectroscopy) spectra were obtained in an ultrahigh vacuum system (10^{-10}-mbar range) with an hemispherical energy analyzer, by using an He discharge lamp (He I, $\hbar\omega = 21.2$ eV); the instrumental resolution was about 0.3 eV. The photon beam had an incidence angle of 45° with respect to the normal at the sample surface.

The main advantage of XPS over UPS is that it directly reflects the density-of-states structure of the filled bands alone, although the latter technique has better resolution. The final state of the photoexcited electrons lies in a region of the empty band structure (~ 1485 eV above the Fermi energy), where there is no density of states modulation.

In the case of $CrCl_3$, due to the insulator nature of the sample, the surface was charged up during the photoemission measurements. However, it did not distort too much the spectral line shape, but it did prevent a precise determination of the Fermi level in the XPS spectra. Therefore, since the origin of the zero binding energies is difficult to determine, we have taken the origin at the top of the valence band.

Photoconductivity was observed at 300 K with monochromatic light parallel to the crystallographic c axis of the compound and chopped at a frequency of 30 Hz. The electrical contacts were made using Ag paste, and photoconductivity experiment masks were used in order to exclude photovoltaic contributions to the measured signal. The photocurrent obtained in the sample and developed across the dark resistance of a second crystal carefully protected from light was amplified and then fed into a HR-8 P.A.R. phase sensitive detector.

III. RESULTS AND DISCUSSION

A. $3d^3$, $CrCl_3$

Figure 2 shows the XPS spectrum of $CrCl_3$ crystals versus the binding energy. The location and identities of the observed spectral features, that is, the valence band, Cr, and Cl core levels are shown. The multiplet splitting of the Cr 3s and 3p core levels is clearly observable: the Cr 3s state, for example, is split by exchange interaction in two peaks located at 75 and 79.5 eV. In order to understand the origin of the splitting we recall that in photoemission experiments one measures the difference in energy between the ground state and the singly ionized state. If an ion has an unfilled 3d shell, the hole created through photoionization can couple to the spin and orbital angular momentum of the unfilled shell and produce multiplet splitting. In an insulator the photohole is well localized, thus it can safely be assumed that the state produced by the coupling of the hole to the open configuration lives long enough to be detected as a final state.

In $CrCl_3$, for example, the three 3d electron spins couple parallel in the Cr^{3+} ion, corresponding to a ground state ^4F in the Russel-Saunders coupling ($S = \frac{3}{2}, L = 3$). By ejecting a Cr 3s electron two final states are possible: $3s3d^3\,{}^3F$ ($S = 1, L = 3$) or $3s3d^3\,{}^5F$ ($S = 2, L = 3$). The basic difference between these final-state configurations is that in the ^3F state the spin of the remaining 3s electron is coupled antiparallel to those of the three 3d electrons, whereas in the ^5F state the 3s and 3d spins are coupled parallel. The ^5F state will be energetically lowered for Hund's rule, favoring the parallel spin exchange interaction: the magnitude of the energy separation (about 4.5 eV) is proportional to the 3s-3d exchange integral. The line intensity ratio is approximately governed by the multiplet ratio $^5F{:}{}^3F = 5{:}3$ and agrees with the observed value.

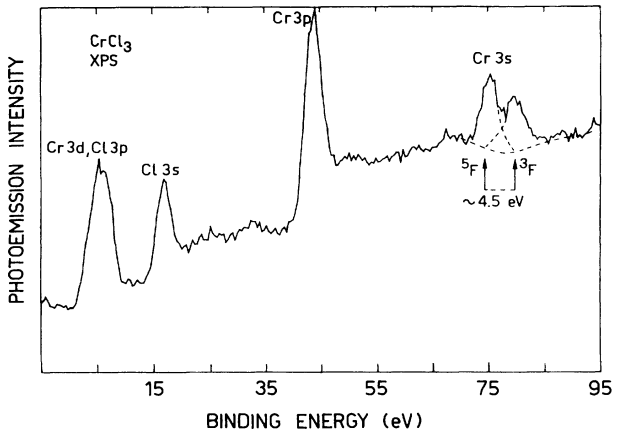

FIG. 2. The energy spectrum of electrons from 1.49-keV photon irradiation-Al $K\alpha$ of chromium chloride. The energy axis is in terms of binding energy, while the vertical axis denotes the rate of counting.

For the Cr 3p photoelectron emission, the number of allowed final states increases for the 3p hole because of the angular momentum ($L = 1$), but the individual shape and intensity of the observed structure is less pronounced as compared to the 3s doublet splitting.

Figure 3 shows the x-ray photoemission valence-band spectrum of $CrCl_3$ at room temperature. The valence band consists of overlapping Cl 3p and Cr 3d states: the Cr 3d band is separated from the underlying Cl 3p band by about 2.5 eV. The experimental bandwidth of the anion p band is about 3 eV, somewhat smaller than its theoretical value W_P due to translational symmetry ($W_P = 4.6$ eV).[11] The width of the d band is about 2.6 eV before correction for instrumental resolution. Its estimated bandwidth (~ 2 eV) is larger than expected on the basis of instrumental and lifetime broadening (localized d orbitals in oxides and halides of transition metals are about 1–1.5 eV wide) and much larger than the one-electron dispersional band width $W_d < 0.3$ eV.[11]

The peak assignments are reported on the ground of a self-consistent, one-electron band-structure calculation: the arrows mark the upper and lower limits of the Cr 3d, Cl 3p, and Cl 4s bands. Although intra-atomic exchange and electron-electron correlation effects between d electrons are not taken into account properly by band theory, it is surprising to note that the theoretical results are able

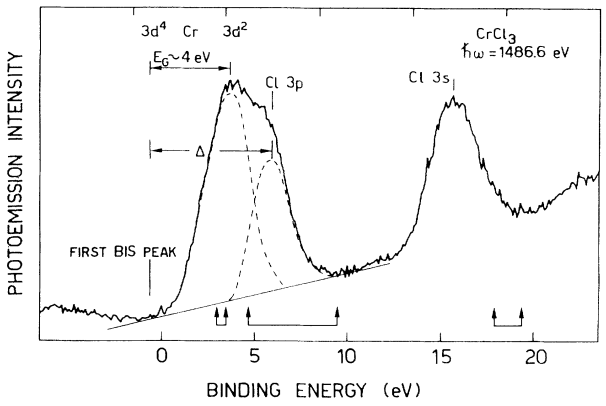

FIG. 3. X-ray photoemission valence-band spectrum of $CrCl_3$ at room temperature. The position of the first bremsstrahlung isochromat spectroscopy (BIS) peak is extrapolated from optical data (Ref. 2). The arrows mark, from left to right, the upper and lower limits of the Cr $3d$, Cl $3p$, and $3s$ bands, respectively, resulting from one-electron band calculations (Ref. 11). The band structure has been shifted rigidly to make the highest occupied d band coincident with the main d emission structure.

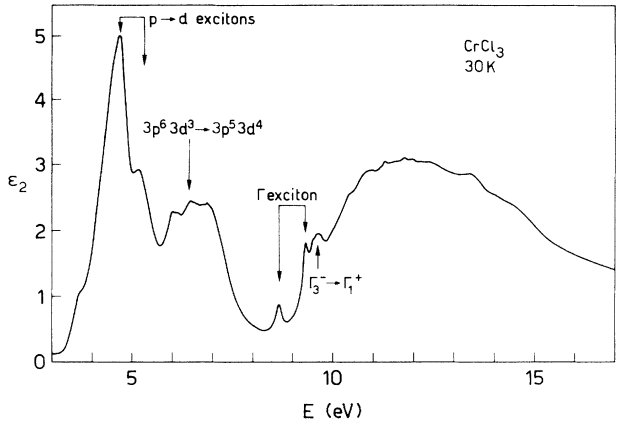

FIG. 4. Imaginary part of the dielectric function of $CrCl_3$ at low temperature together with the proposed assignments: charge transfer excitons and transitions are indicated around 5 and 6.5 eV. The interband transition at 9.7 eV is shown: this occurs at Γ between the top of the valence band p and the bottom of the s conduction band (Ref. 2).

to predict the experimental spectrum rather well with regard to the band positions, if we except the position of the lower lying $3s$ band. However, no agreement is found with the observed insulating character of the compound: one must then think that the electron-electron correlation introduces an energy gap in the $3d$ states, which can explain the insulating character of the material.

Let us now discuss the nature of the energy gap E_G, that is whether $CrCl_3$ presents a d-d (Mott-Hubbard regime) or p-d (charge-transfer regime) gap.

In Fig. 3, the spectral feature extending from 4 to 9 eV is associated with chlorine $3p$ valence states, while the structure around 3 eV is assigned to a localized Cr $3d^2$ hole state as in the case of Cr_2O_3,[5] which has been classified as a MH insulator on the basis of resonant photoemission.[33]

Thus, the energy gap E_G is ascribed to $d \rightarrow d$ intercationic transitions and one can assign the final-state structure of the high spin Cr in $CrCl_3$ in terms of the $3d^2$ final-state ionization potentials. The trivalent Cr ion has three electrons in the $^4A_2$ configuration, i.e., coupled spins parallel in a weak octahedral field (Hund's rule): upon photoionization one observes one single final state, $^3T_1$, somewhat broadened by p-d hybridization ($\simeq 2$ eV).

In order to give an estimation of the correlation energy U one should know the energy position of the $3d^4$ states, which we can approximately evaluate by considering the charge transfer transitions $3p^6 3d^3 \rightarrow 3p^5 3d^4$, occurring around 6.5 eV in the optical spectrum of $CrCl_3$ shown in Fig. 4: we can thus predict that the first inverse photoemission peak $3d^4$ will be located around 4 eV above the d-emission peak. In Fig. 3 we can also give an estimate of $U \simeq 4$ eV for Cr in $CrCl_3$: it is interesting to note that the value $U \simeq 4$ eV and $\Delta \sim 6.5$ eV in $CrCl_3$ are not too far from the values estimated for Cr in Cr_2O_3: $U = 3.3$ eV and $\Delta = 6.3$ eV (see Table I of Ref. 34). The approximately 4 eV separation between the d^2 and d^4 configurations reflects the size of U: taking into account the uncertainties of the ground- and final-state hybridization shifts, we believe that 2.8–3 eV is a fair estimate of U. The dispersional width of the d band of the metal ion, which is usually small ($W_d < 0.3$ eV), is not taken into account.

In conclusion, while the feature extending from 4 to 9 eV is due to the Cl $3p$ valence-band states, the peak around 3 eV, the so-called main d emission, has been assigned to the $3d^2$ final states, produced by the emission of a $3d$ electron from the $3d^3$ ground state. No satellite emission was observed in the photoelectron spectrum of $CrCl_3$.

B. $4d^5$, α-$RuCl_3$

In Fig. 5 the XPS spectrum of $RuCl_3$ is shown. The observed spectral features can be grouped into two basic types, that is, peaks due to photoemission from core levels and valence states. The sidebands located at high binding energy of the Cl $2p$ and Ru $3d$ core levels are attributed to collective valence electron oscillations (plasmons). We can also note that core levels have variable intensities and widths and that the non-s-levels are doublets. The doublets Ru $3d$ and $3p$ arise through the spin-orbit coupling (jj) and the difference in energy of the states reflects the "parallel" or "antiparallel" nature of the spin and orbital angular momentum vectors of the remaining electron.

The XPS and UPS valence-band spectra of $RuCl_3$ measured at room temperature are presented in Figs. 6 and 7, respectively. They are formed by three resolved bands originated from the Ru $4d$ and Cl $3p$ states: the highest band with a broadening of 1.5 eV (XPS) and 1 eV (UPS) (full width at half maximum) is primarily of d symmetry,

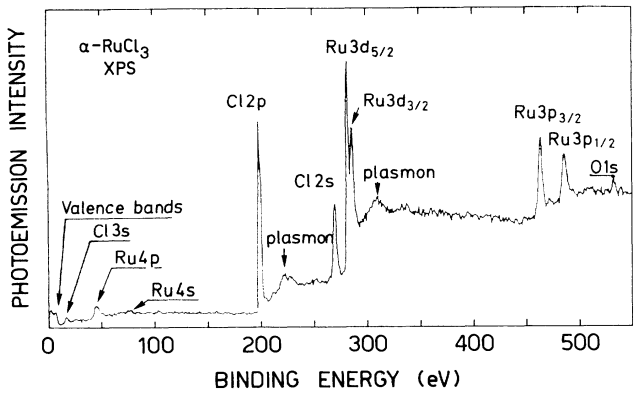

FIG. 5. The energy spectrum of electrons from the 1.49 keV photon irradiation (Al $K\alpha$) of ruthenium chloride. The energy axis gives the binding energy; the vertical axis denotes the rate of counting.

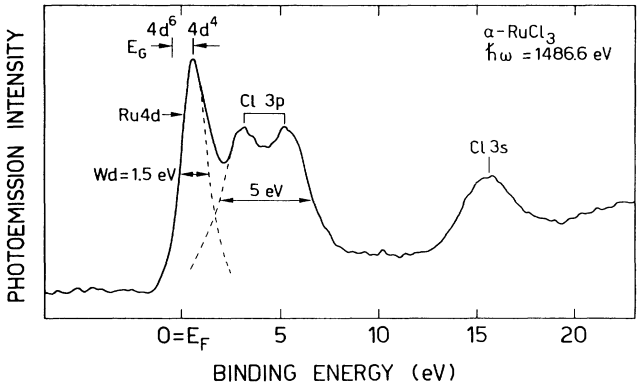

FIG. 6. X-ray photoemission valence-band spectrum of α-$RuCl_3$ crystals. E_F is the Fermi level and E_G indicates the photoconductivity energy gap at 300 K.

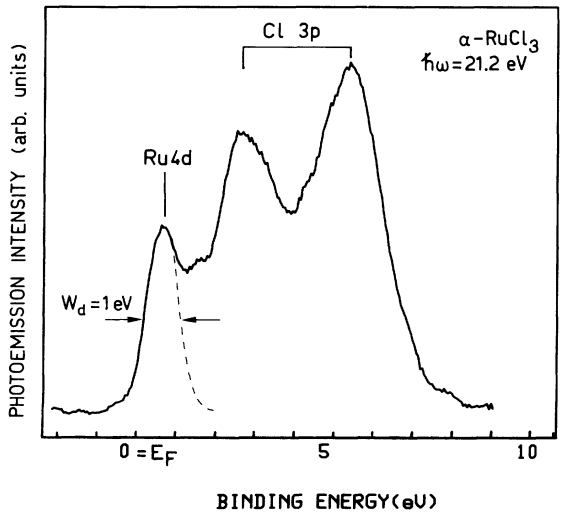

FIG. 7. Angle-resolved ultraviolet photoemisson spectrum of the valence bands of α-$RuCl_3$ at normal emission.

while the higher binding-energy bands (from 2.5 to 8 eV) are mainly of p symmetry. This is indicated by the strong intensity increase of the uppermost narrow band with respect to the lower energy bands extending up to 8 eV. This effect is mainly due to the strong dependence of the valence-band photoionization cross sections with the increase of the photon energy: it has been observed in TMC and TM oxides[5] and also in chalcogenides[35] and halides.[36] One can also notice that the intensity of the p band located at 3 eV in the UPS spectrum increases, together with the intensity of the Ru 4d band, with the photon energy and that in the XPS spectrum has the same intensity of the 6-eV peak: this fact can be explained by considering that some degree of p-d hybridization is present in this material.

Let us now discuss the photoemission spectra of $RuCl_3$, together with the photoconductivity and reflectance data presented in Figs. 8 and 9, respectively.

In the photoconductivity spectrum of $RuCl_3$ (Fig. 8) the spectral distribution of the photocurrent shows a threshold around 1 eV, followed by a knee at 1.20 eV and a broad maximum around 2.10 eV. The photoconductivity edge, in close correspondence with the reflectance peak observed at 1.1 eV, gives the experimental value of the conductivity energy gap of the compound. Below 1 eV, low-energy absorption features (0.28, 0.53, and 0.75 eV) are due to spin-forbidden intracationic transitions.[25]

$RuCl_3$ is a low-spin compound with a high crystal field, and the optical transitions in the energy range 0.9–2.5 eV, leading to photoconductivity, are better interpreted in terms of spin-allowed d-d in terms of spin-allowed d-d excitations for the low-spin d^5 configuration. The reflectivity spectral feature at 1.1 eV is then assigned to a spin-allowed d-d transition ($^2T_2 \rightarrow {}^2A_2, {}^2T_1$) responsible for the absorption edge and the photoconductivity threshold. In turn, the 5.2-eV peak is attributed to a charge-transfer transition from an initial state of predominantly halogen character to an empty d level. Metal 5s levels, permitting band-to-band transitions, only become available for transitions greater than 7.8 eV (see Fig. 9).

This is also in agreement with the results of the photo-

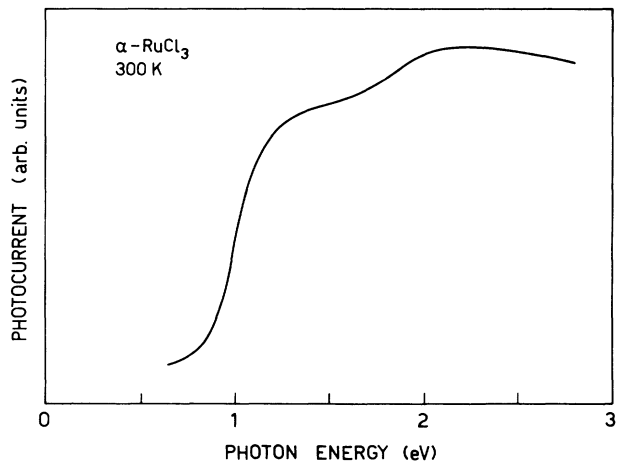

FIG. 8. Photoconductivity spectrum of $RuCl_3$ at 300 K, using Ag as contact material.

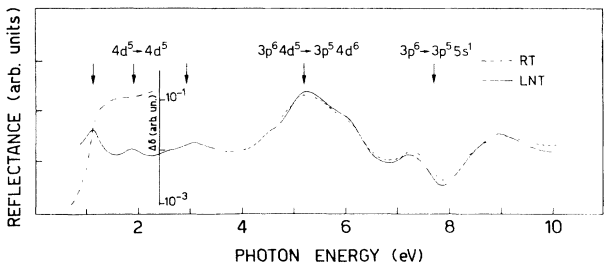

FIG. 9. Reflectivity spectrum of $RuCl_3$ at 80 and 300 K. Room-temperature photoconductivity is reported for comparison, and the proposed assignments are indicated. Arbitrary units are used throughout.

emission data. The XPS and UPS spectra of $RuCl_3$ can be divided into Cl $3p$- and Ru $4d$-derived features. The Ru $4d$ band lies above the Cl $3p$ valence band by about 2.5 and 2 eV, respectively, and no multielectron satellite was observed (see Figs. 6 and 7). The main d emission is assigned to an unscreened $4d^4$ hole state produced by the emission of a $4d$ electron from the Ru $4d^5$ ground state ($^2T_2$). The energy gap E_G, ascribed to d-d transitions, is

$$E_G = U - W_d/2 ,$$

where U is the Coulomb correlation energy and W_d is the Ru $4d$ energy bandwidth.

In particular, a recent angle-resolved photoemission (ARP) study of $RuCl_3$ supports a localized description of the $4d$ orbitals since little dispersion (<0.2 eV) of the d bands was observed.[37] Moreover, with photoconductivity measurements (Fig.8), one determines the conductivity energy gap (which is the difference between the ionization potential and the electron affinity of the solid) unambiguously since exciton absorption will not contribute to the photocurrent. Thus, the value of the photoconductivity edge (about 1 eV) giving the separation between d^4 and d^6 configurations, approximately reflects the size of the Mott-Hubbard gap U, if one neglects the value of $W_d < 0.2$ eV (see Fig. 6). The assignment of the valence band $4d$ emission to a $4d^4$ final state structure, as indicated by the foregoing experimental results on $RuCl_3$, is in line with the assumption of correlation-localized $4d$ electrons in the ground state (MH insulator).

Such a model is appropriate when the ratio $U/W_d > 1$ and gives for $RuCl_3$ a ratio $U/W_d > 4.5$. The estimate of this ratio for $CrCl_3$ (about 10) is less precise, because the experimental determination of the energy gap is not easy; the theoretical value of W_d is obtained on the ground of a one-electron band calculation.

With regard to the photoconductivity excited in the energy range (below 3 eV) of d-d transitions, we think that a hopping type of conduction should take place in which the electron would diffuse from one cation site to the next. The intrinsic ionization energy E_G would then represent the energy required to create an electron-hole pair, that is, Ru^{2+} and Ru^{4+} ions. The following reaction shows the way this could happen:

$$Ru^{3+}(4d^5) + Ru^{3+}(4d^5) \rightarrow Ru^{2+}(4d^4) + Ru^{4+}(4d^6) .$$

This shows the formation of a conduction electron and hole in the $4d$ Hubbard bands analogously to what was observed in Fe_2O_3 and NiO.[38] In $RuCl_3$ a current can be carried if Ru^{2+} and Ru^{4+} ions are present. These electronic configurations can move through the lattice with a definite wave number for the wave function, just as an electron, hole, or exciton can. The outstanding characteristic of many of these insulators is their very low carrier mobility (below 10^{-2} $cm^{-1}V^{-1}s^{-1}$), which has been interpreted as indicating a "hopping process" conduction mechanism.

Beside the study of the electrical conductivity of intrinsiclike samples, another technique which could verify the nature of the band gap in TMC is resonant photoemission from the valence band and core levels. Photoemission satellites have been observed in Ni oxides and halides,[8,17] in CoO,[10] and also MnO.[9] In all these cases resonant photoemission has suggested that the satellites are due to $3d^{n-1}$ final states and that the main bands are due to ligand-to-$3d$ charge-transfer final states. Fujimori and Minami,[8] and Davis[39] found that the d^{n-1} final states exhibit a Fano-like resonant behavior, whereas any final state involving a ligand hole exhibits a much weaker antiresonant behavior in agreement with experiment.[40,41] Resonant photoemission measurements have also been performed on early $3d$ TM oxides, such as Ti_2O_3 and V_2O_3, which have been classified as MH insulators.[6,42-43]

C. $4d^4$, RuO_2

Spectra of $RuCl_3$ and RuO_2 have been reported by Mc Evoy[30] and in general show the same gross features, although the p-like valence bands are not resolved. In Table I the core level energies for $RuCl_3$, RuO_2, and Ru metal are reported.[30,44]

It is interesting to discuss the XPS valence-band spectrum of $RuCl_3$ (semiconductor) with that of RuO_2 (metal)[45] in view of the similarity of the photoemission spectra and different electrical behavior. The knowledge of the valence-band structure and density of states curves of RuO_2 (Ref. 46) together with the measurement of the dispersion of the d and p bands of $RuCl_3$ (Ref. 38) allow some insight into the electronic structure of $RuCl_3$ and the electric properties of the two materials. We consider the valence-band photoemission spectrum of RuO_2 presented in Fig. 1 of Ref. 45 and the calculated density-of-state curves shown in Fig. 7 of Ref. 46. One observes an energy separation of about 2.2 eV between the metal atom $4d^4$ band and the oxygen $2p$ bands: the value of the p-d separation is close to the measured value, once the instrumental resolution is taken into account. However, the metal-oxygen covalency overlap interactions are important in determining the width of the valence and conduction bands, in particular, it is shown that most of the $4d$ bandwidth arises from the overlap interactions of the t_{2g} and e_g orbitals with the O $2p$ bands. Thus, the Ru $4d$ states broaden into a dispersive, partly filled band, where metallic conduction is possible (see also Fig. 2 of Ref. 46).

In Figs. 6 and 7 one can observe that in $RuCl_3$ the peak-to-peak distance between the Ru $4d^5$ band and the uppermost Cl $3p$ band is of the same order of magnitude

as in RuO_2, that is, 2–2.5 eV. $RuCl_3$, however, is not a metal: thus in $RuCl_3$ the covalency-overlap interactions in the initial ($4d^5$) or final ($4d^4$) states do not seem strong enough for the formation of itinerant (bandlike) $4d$ states. This is confirmed by the results of ARP spectra, which show disperless Ru $4d$ bands[37] along the important symmetry lines of the Brillouin zone. This fact suggests that the $4d$ states remain quite localized and that the metallic conduction in the $4d$ narrow band is not possible, although the $4d$ shell is partially filled: the presence of the energy gap prevents the material to become metallic.

As for the similarity between photoemission spectra of RuO_2 (d^4) and $RuCl_3$ (d^5) a comment can be made. Although the photoemission experiments measure the difference in energy between the ground state and the photoionized state, in a metal, with many electrons around, one may envision that the hole in the valence band is readily screened so that practically no final-state interaction is observed. In the case of an XPS spectrum the intensity of the photoelectron ejected from filled levels will be a convolution of the filled and empty density of states (DOS) of a continuum so that the observed DOS closely reflects the initial filled density of states. In this sense, the main photoemission spectrum of RuO_2 reflects the d emission of the screened Ru $4d^4$ hole and the p-valence band of oxygen, with a measured p-d separation of about 2.2 eV. In the case of $RuCl_3$ instead we observe the photoemission of the Ru $4d^4$ orbitals near the top of the Cl $3p$ valence band, that is the final-state $4d^4$ configuration due to an unscreened valence-band hole. Since $RuCl_3$ is a low-spin complex with a d^5 ground-state configuration ($^2T_2$) we can observe only one photoionized band. The measured peak-to-peak distance in $RuCl_3$ is about 2.5 eV in the XPS spectrum (Fig. 6) and 2 eV in the UPS spectrum (Fig. 7).

Although the spectra are qualitatively similar, the energy positions of the correspondent bands in $RuCl_3$ and RuO_2 are not the same: the difference arises in a compli-

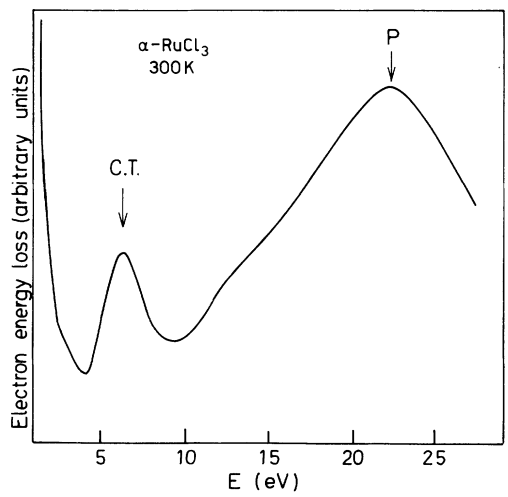

FIG. 10. Characteristic electron energy-loss spectrum of α-$RuCl_3$ crystals measured at room temperature. The energy losses marked CT and P are associated with charge-transfer transitions and valence-electron plasma oscillations, respectively.

TABLE I. Binding energy (eV) of core levels for $RuCl_3$, RuO_2, and Ru metal.

Identification	Cl 3s (eV)	O2s (eV)	Ru $4p_{3/2}$ (eV)	Ru $4p_{1/2}$ (eV)	Ru 4s (eV)	Cl $2p_{3/2}$ (eV)	Cl $2p_{1/2}$ (eV)	Cl 2s (eV)	Ru $3d_{5/2}$ (eV)	RU $3d_{3/2}$ (eV)	Ru $3p_{3/2}$ (eV)	Ru $3p_{1/2}$ (eV)	O 1s (eV)	Ru 3s (eV)
$RuCl_3$ (single crystal) (this work)	15.6		44	45.4	75.7	197.6	199.1	268.8	281	285.4	462.5	484.8		586.8
$RuCl_3$ (powder) [McEvoy (Ref. 30)]	15.7			44.6	75.9	197.8		268.7	280.8	284.9	462.3	484.6		587.2
RuO_2 (powder) [McEvoy (Ref. 30)]		21.4		44.8	76.1				280.7	284.8	462.3	484.7	530.8	588.0
Ru (single crystal) [Fuggle (Ref. 44)]		43.2		46.5	75.0				279.9	284.1	461.2	483.3		586.6

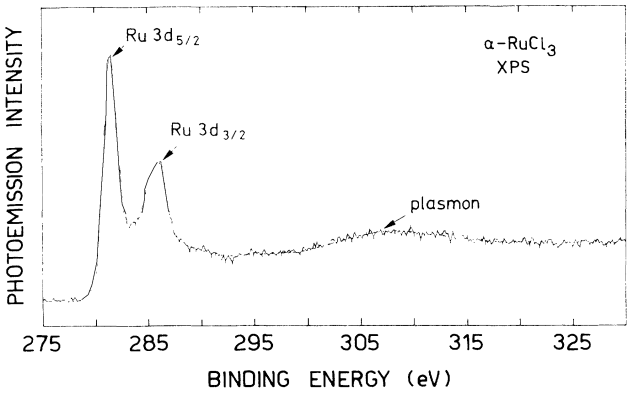

FIG. 11. X-ray photoemission spectrum of Ru $3d$ core levels split by spin-orbit coupling. The broad band separated from the atomic levels of Ru by about 24 eV is attributed to a valence-band plasmon.

cated way from the details of the crystals potential and the filling of the d bands.

In Fig. 10 we have finally shown the electron energy-loss spectrum of $RuCl_3$ performed with a spectrometer where a monoenergetic electron beam (50 keV) is transmitted through the crystalline specimen. Optical charge transfer transitions cause a strong energy loss peak with a maximum around 6.25 eV. A weak shoulder, clearly observable below 4 eV, should be due to the relatively strong spin-allowed crystal-field transitions. The strong band reaching its maximum at 22.3 eV confirms the presence of collective oscillations due to the valence electrons ($4d$, $3p$, and $3s$). In Fig. 11, the XPS spectrum of the $3d_{3/2}$ and $3d_{5/2}$ core levels of ruthenium shows a weak and broad sideband still associated with valence electron plasma oscillations of energy around 24 eV. The same plasmon structure is also observed in connection with the Cl $2p$ core levels (see Fig. 5).

IV. CONCLUSIONS

XPS and UPS valence-band measurements of two typical $3d$ and $4d$ transition-metal compounds, $CrCl_3$ and $RuCl_3$, have permitted us to determine basic parameters such as the transition-metal d level position and width, as well as the energy separation of the d states from the ligand $3p$ bands. It is shown that the $3d$ and $4d$ states of the chromium and ruthenium atoms and the $3p$ states of the chlorine contribute to the formation of the valence band in these materials.

Photoemission results have then been compared with photoconductivity and optical data in order to discuss the origin of the energy gap of these transition-metal halides with open d-shell configuration. The Cr $3d$- and Ru $4d$-derived structures near the top of the Cl $3p$ valence band come from unscreened (or poorly screened) $3d^2$ holes in $CrCl_3$ and $4d^4$ holes in $RuCl_3$. Both compounds are classified as Mott-Hubbard insulators in which the band gap corresponds to intercationic d-d transitions. The estimated value of the d-d Coulomb correlation energy is $U=2.8-3$ eV for $CrCl_3$ and $U=1$-1 eV for $RuCl_3$. In $RuCl_3$ the photoconductivity threshold and the optical absorption edge around 1 eV give the experimental value of the conductivity energy gap. It is suggested that the energy gap in this compound is due to an intersite hopping transition within the framework of the Hubbard Hamiltonian. An alternative possibility is a delocalized d-d transition involving more than one site.[47]

In particular, the comparison with RuO_2 and the experimental data on $RuCl_3$ strongly suggest that an insulating gap exists in the paramagnetic phase of $RuCl_3$ and that the $4d$ levels are strongly localized, forming a very narrow band with a ARP dispersion band width <0.2 eV. Although a full understanding of the data awaits further experimental and theoretical work on these highly correlated materials, is seems that the present results can be described within a Mott-Hubbard model which is appropriate when $U/W_d>1$.

ACKNOWLEDGMENTS

This investigation was supported in part by the Consorzio Interuniversitario Nazionale per la Fisica della Materia (INFM). The author is much obliged to the technical staff of the ESCA apparatus of the "Ecole Nationale Supérieure de Chimie de Toulouse" and the "Service de Microscopie Electronique" of Paul Sabatier University (Toulouse). He would also like to thank B. Carricaburu and R. Mamy for experimental help in connection with the photoemission measurement, and for interesting discussions.

[1]Y. Sakisaka, T. Ishii, and T. Sagawa, J. Phys. Soc. Jpn. **36**, 1365 (1974); **36**, 1372 (1974).
[2]B. Carricaburu, J. Ferrè, R. Mamy, I. Pollini, and J. Thomas, J. Phys. C **19**, 4885 (1986); I. Pollini, J. Thomas, B. Carricaburu, and R. Mamy, J. Phys. Condens. Matter **1**, 7695 (1989).
[3]C. R. Ronda, G. J. Arends, and C. Haas, Phys. Rev. B **35**, 4038 (1987).
[4]J. Thomas, G. Jezequel, and I. Pollini, J. Phys. Condens. Matter **2**, 5439 (1990).
[5]D. E. Eastman and J. L. Freouf, Phys. Rev. Lett. **34**, 395 (1975).
[6]S. Hüfner and G. K. Wertheim, Phys. Rev. B **8**, 4857 (1973).
[7]S. Hüfner, Solid State Commun. **53**, 707 (1985).
[8]A. Fujimori and F. Minami, Phys. Rev. B **30**, 957 (1984); A. Fujimori, F. Minami, and S. Sugano, *ibid.* **29**, 5225 (1984).
[9]R. J. Lad and V. E. Heinrich, Phys. Rev. B **38**, 10 860 (1988).
[10]Z. X. Shen, J. W. Allen, P. A. P. Lindberg, D. S. Dessau, B. O. Wells, A. Borg, W. Ellis, J. S. Kang, S. J. Oh, I. Lindau, and W. E. Spicer, Phys. Rev. B **42**, 1817 (1990).
[11]S. Antoci and L. Mihich, Phys. Rev. B **18**, 5768 (1978).
[12]S. Antoci and L. Mihich, Phys. Rev. B **21**, 3383 (1980).
[13]N. F. Mott, Proc. Phys. Soc. (London) Sec. A **62**, 416 (1949); Can. J. Phys. **34**, 1356 (1956); Philos. Mag. **6**, 287 (1961).
[14]J. Hubbard, Proc. R. Soc. London Ser. A **276**, 238 (1963); **277**, 237 (1964); **281**, 401 (1964).
[15]W. Albers and C. Haas, Phys. Lett. **8**, 300 (1964).
[16]G. A. Sawatzky and J. W. Allen, Phys. Rev. Lett. **53**, 2339 (1984).

[17]G. A. Sawatzky, in *Core Level Spectroscopy in Condensed Systems*, edited by J. Kanimori and A. Kotani (Springer-Verlag, Berlin, 1988), p. 99.
[18]J. Zaanen, G. A. Sawatzky, and J. W. Allen, Phys. Rev. Lett. **55**, 418 (1984); J. Magn. Magn. Mater. **54-57**, 607 (1986).
[19]J. Zaanen, C. Westra, and G. A. Sawatzky, Phys. Rev. B **33**, 8060 (1986).
[20]S. Hüfner, J. Osterwalder, T. Riesteder, and F. Hulliger, Solid State Commun. **52**, 793 (1984).
[21]S. Hüfner and T. Riesteder, Phys. Rev. B **33**, 7267 (1986).
[22]J. W. Cable, M. K. Wilkinson, and E. O. Wollan, J. Phys. Chem. Solids **19**, 29 (1961).
[23]B. Morosin and A. Narath, J. Chem. Phys. **40**, 1958 (1964).
[24]G. Guizzetti, E. Reguzzoni, and I. Pollini, Phys. Lett. **70**, A34 (1979).
[25]L. Binotto, I. Pollini, and G. Spinolo, Phys. Status Solidi B **44**, 245 (1971).
[26]J. M. Fletcher, W. E. Gartner, A. C. Fow, and G. Topping, J. Chem. Soc. (A) 1038 (1967).
[27]J. O. Williams and T. Mahmood, Appl. Surf. Sci. **6**, 62 (1980).
[28]W. D. Jonhston, H. J. Leany, B. A. Parkinson, A. Heller, and B. Miller, J. Electrochem. Soc. **127**, 90 (1980).
[29]S. Pizzini, G. Buzzanca, C. Mari, L. Rossi, and S. Torchio, Mater. Res. Bull. **7**, 449 (1972).
[30]A. J. Mc Evoy, Phys. Status Solidi A **71**, 569 (1982).
[31]J. M. Fletcher, W. E. Gardner, E. W. Hooper, K. R. Hyder, and J. L. Woodhead, Nature **199**, 1089 (1963).
[32]F. Hulliger, in *Structural Chemistry of Layer-Type Phases. Physics and Chemistry of Materials with Layered Structure*, edited by F. Levy (Reidel, Dordrecht, Holland, 1976), Vol. 5.
[33]X. Li, L.Liu, and V. E. Henrich, Solid State Commun. **84**, 1103 (1992).
[34]J. Zaanen and G. A. Sawatzky, J. Solid State Chem. **88**, 8 (1990).
[35]I. T. Mc Govern and G. H. William, J. Phys. C **9**, L337 (1976).
[36]A. Goldman, J. Tejeda, N. J. Shevchik, and M. Cardona, Phys. Rev. B **10**, 4388 (1974).
[37]B. Carricaburu, R. Mamy, and I. Pollini (unpublished).
[38]F. J. Morin, Phys. Rev. **93**, 1195 (1954); **93**, 1199 (1954).
[39]L. C. Davis, Phys. Rev. B **25**, 2912 (1982); **25**, 2912 (1982).
[40]S. J. Oh, J. W. Allen, I. Lindau, and J.C. Mikkelsen, Jr., Phys. Rev. B **26**, 4845 (1982).
[41]M. R. Thuler, R. L. Benbow, and Z. Hurych, Phys. Rev. B **27**, 2082 (1983).
[42]S. Shin, S. Suga, M. Taniguchi, M. Fujisawa, H. Kanzaki, A. Fujimori, H. Daimon, Y. Ueda, K. Kosuge, and S. Sachi, Phys. Rev. B **41**, 4993 (1990).
[43]Z. Zhang, S. P. Jeng, and V. E. Heinrich, Phys. Rev. B **43**, 12 004 (1991).
[44]J. C. Fuggle, T. E. Madey, M. Steinkilberg, and D. Menzel, Surf. Sci. **52**, 521 (1975).
[45]N. Beatham and A. F. Ochard, J. Electron Spectrosc. Relat. Phenom. **16**, 77 (1979).
[46]L. F. Mattheiss, Phys. Rev. B **13**, 2433 (1976).
[47]C. H. Maule, J. N. Tothill, P. Strange, and J. A. Wilson, J. Phys. C **21**, 2153 (1988).

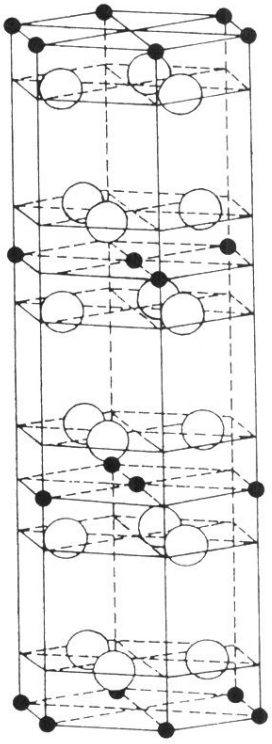

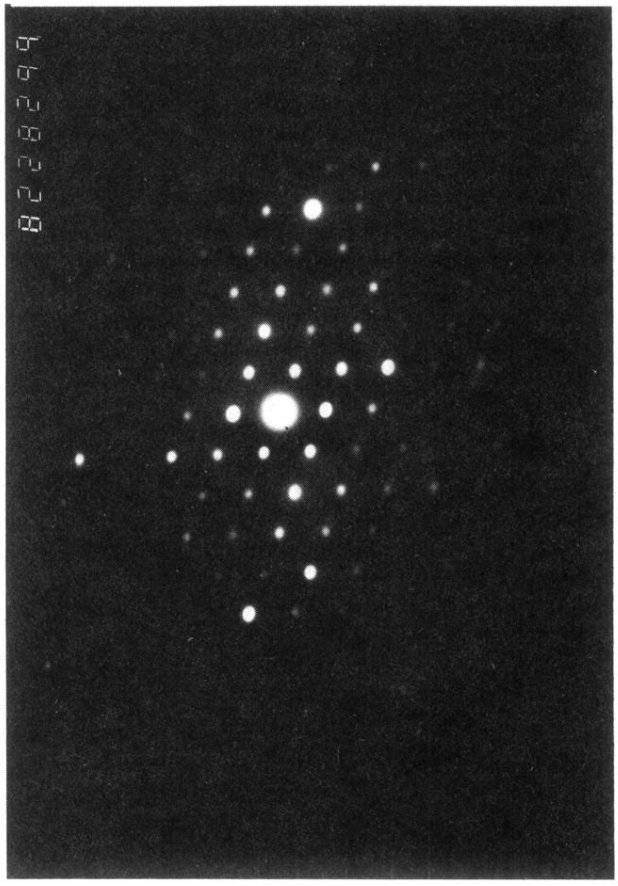

FIG. 1. High-energy (200 kV) electron Bragg diffraction patterns of crystals of α-$RuCl_3$. The monochromatic electron beam was incident on the crystal surface along the c axis. In the inset the structure of $CrCl_3$ and $RuCl_3$ crystals shows the octahedral environment of the metal (●, Cr, Ru; ○, Cl).